第 15 卷第 6 期 2017 年 12 月
1672-6553/2017/15(6)/489-5

动力学与控制学报
JOURNAL OF DYNAMICS AND CONTROL

Vol.15 No.6
Dec. 2017

受电压激励的复合材料悬臂板的分叉分析*

杨佳慧[1,2]　张伟[1†]　姚明辉[1]

（1.北京工业大学机电学院,北京　100124）（2.北京农业职业学院,北京　102208）

摘要　以飞行器机翼作为工程背景,将机翼简化为悬臂板模型,研究了受横向电压激励、基础激励、面内激励联合作用下复合材料层合悬臂板的非线性动力学问题.首先建立其动力学模型,考虑冯-卡门大变形理论,利用 Hamilton 原理建立复合材料层合悬臂板的非线性动力学方程;选择符合边界条件的模态函数,利用 Galerkin 方法对系统进行四阶离散,得到四自由度非线性常微分方程;代入系统实际物理参数,应用MATLAB 软件数值模拟得到系统振动幅值随电压激励变化的分叉图,由图可知,电压激励使系统从混沌运动变为倍周期运动,降低了系统振幅,保持系统的稳定.

关键词　悬臂板,　Hamilton 原理,　分叉,　非线性动力学,　混沌

DOI:　10.6052/1672-6553-2017-56

引言

压电效应是 1880 年 Curie 兄弟发现的.压电材料的正压电效应即通过施加外作用力,使压电材料变形,从而输出电能,一般用做能量采集器.压电材料的逆压电效应是在外电场作用下压电材料产生形变,从而抑制系统振动.常用的压电材料有压电陶瓷类(PZT)和压电薄膜类(PVDF).压电陶瓷较脆,在电场激励下所能产生的驱动力有限.压电薄膜轻而柔软,易加工成型,可应用于梁、板、壳及复杂形面结构.压电材料成本低廉、生产工艺比较成熟[1].

2001 年,Zhang[2,3] 等分别研究了面内激励作用下四边简支矩形板以及面内激励和横向外激励联合作用下四边简支矩形板的非线性动力学.2008 年,Hao[4] 等利用高阶板壳理论研究了面内激励和横向外激励联合作用下四边简支矩形功能梯度板的非线性动力学行为.2009 年,Yao[5] 等对压电复合材料层合简支梁进行了混沌动力学与控制研究.

2011 年,Inman[6] 等研究了无人机上的能源采集器,在无人机的机翼上嵌入压电陶瓷,利用气动载荷使压电材料振动发电,机翼的力学模型是悬臂压电板结构.2013 年,Inman[7] 等用实验方法研究了双稳态层合压电板结构,给出了低频振动、不均匀的跳变和重复均匀跳变时的时间历程图和二维相图.2016 年,李蒙[8] 等以复合材料悬臂板为主要研究对象,研究了其振动主动控制及控制器铺设位置的优化问题.

以上文献建立的动力学模型多为简支板模型,悬臂板较少,且最多为三阶离散,本文以飞行器机翼为工程背景,建立受电压激励、基础激励、面内激励联合作用下复合材料层合悬臂板的力学模型,应用 Hamilton 原理及 von Karman 大变形板理论,对系统进行四阶 Galerkin 离散,得到四自由度非线性动力学方程,分析了受电压激励时,复合材料层合悬臂板的非线性动力学响应.

1　基本方程

建立复合材料层合悬臂板的力学模型如图 1 所示.悬臂板由三层材料组成,中间为基底层,材料选用石墨/环氧(HT3/QY8911)树脂,上下两层为压电薄膜(PVDF)层.悬臂板总的长、宽、厚分别为 a, b, h,建立直角坐标系在板的中面,板的固定端受基础激励 $F\cos(\Omega_1 t)$ 的作用,横向受电压激励,形式为 $V\cos(\Omega_2 t)$,面内激励为 $p_0+p_1\cos(\Omega_3 t)$.

2016-12-29 收到第 1 稿,2017-01-24 收到修改稿.
* 国家自然科学基金资助项目(11290152,11322214)
† 通讯作者 E-mail: sandyzhang0@ yahoo.com

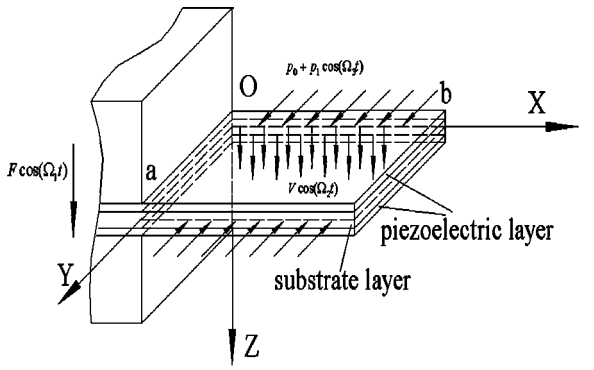

图 1 复合材料层合压电悬臂板的力学模型

Fig.1 Mathematical model of a cantilevered piezoelectric plate structure

根据经典板理论[9],板的任意一点的位移可以写为:

$$\begin{aligned} u_1 &= u(x,y,z,t) = u_0(x,y,t) - z\frac{\partial w_0}{\partial x} \\ u_2 &= v(x,y,z,t) = v_0(x,y,t) - z\frac{\partial w_0}{\partial y} \\ u_3 &= w(x,y,z,t) = w_0(x,y,t) \end{aligned} \tag{1}$$

式(1)中 u_0, v_0, w_0 分别为中面上任意一点沿 x, y, z 方向的位移.

根据 von Karman 非线性应变-位移几何关系,得应变-位移关系:

$$\begin{aligned} &\varepsilon_{xx} = \frac{\partial u}{\partial x} + \frac{1}{2}\left(\frac{\partial w}{\partial x}\right)^2, \varepsilon_{yy} = \frac{\partial v}{\partial y} + \frac{1}{2}\left(\frac{\partial w}{\partial y}\right)^2 \\ &\varepsilon_{zz} = \frac{\partial w}{\partial z}, \varepsilon_{xy} = \frac{1}{2}\left(\frac{\partial u}{\partial y} + \frac{\partial v}{\partial x} + \frac{\partial w}{\partial x}\frac{\partial w}{\partial y}\right) \\ &\varepsilon_{yz} = \frac{1}{2}\left(\frac{\partial w}{\partial y} + \frac{\partial v}{\partial z}\right), \varepsilon_{xz} = \frac{1}{2}\left(\frac{\partial u}{\partial z} + \frac{\partial w}{\partial x}\right) \end{aligned} \tag{2}$$

对于正交铺设的各向异性层合板,其应力-应变的本构方程可以写为:

$$\begin{Bmatrix} \sigma_{xx} \\ \sigma_{yy} \\ \sigma_{yz} \\ \sigma_{zx} \\ \sigma_{xy} \end{Bmatrix} = \begin{bmatrix} Q_{11} & Q_{12} & 0 & 0 & 0 \\ Q_{21} & Q_{22} & 0 & 0 & 0 \\ 0 & 0 & Q_{44} & 0 & 0 \\ 0 & 0 & 0 & Q_{55} & 0 \\ 0 & 0 & 0 & 0 & Q_{66} \end{bmatrix} \begin{Bmatrix} \varepsilon_{xx} \\ \varepsilon_{yy} \\ \gamma_{yz} \\ \gamma_{zx} \\ \gamma_{xy} \end{Bmatrix} - \begin{Bmatrix} e_{31} \\ e_{32} \\ 0 \\ 0 \\ 0 \end{Bmatrix} E \tag{3}$$

其中 e_{ij} 为压电常数,E 为电场强度,弹性刚度系数 Q_{ij} 如下式所示:

$$\begin{aligned} &Q_{11} = \frac{E_1}{1-\nu_{12}\nu_{21}}, Q_{12} = \frac{\nu_{12}E_2}{1-\nu_{12}\nu_{21}}, Q_{21} = Q_{12}, \\ &Q_{22} = \frac{E_2}{1-\nu_{12}\nu_{21}}, Q_{44} = G_{23}, Q_{55} = G_{13}, Q_{66} = G_{12} \end{aligned} \tag{4}$$

其中 $E_i(i=1,2)$ 为单层材料的弹性模量,G_{12} 为单层材料的剪切模量,ν_{12} 和 ν_{21} 为单层材料的泊松比.

根据 Hamilton 原理:

$$\delta\int_{t_1}^{t_2}(T-U)\,dt + \int_{t_1}^{t_2}\delta W\mathrm{d}t = 0 \tag{5}$$

对于压电材料,引入第二类压电本构方程如下:

$$\begin{aligned} T &= Q\varepsilon - eE \\ D &= e\varepsilon + \zeta E \end{aligned} \tag{6}$$

式中 $T, \varepsilon, D, Q, e, E, \zeta$ 分别代表应力、应变、电位移、弹性模量、压电常数、电场强度、介电常数.

代入哈密顿原理,得内力表示的复合材料层合悬臂板的控制方程如下:

$$\begin{aligned} &\frac{\partial N_{xx}}{\partial x} + \frac{\partial N_{xy}}{\partial y} = I_0\ddot{u}_0 - I_1\frac{\partial \ddot{w}_0}{\partial x} \\ &\frac{\partial N_{yy}}{\partial y} + \frac{\partial N_{xy}}{\partial x} = I_0\ddot{v}_0 - I_1\frac{\partial \ddot{w}_0}{\partial y} \\ &\frac{\partial N_{xx}}{\partial x}\frac{\partial w_0}{\partial x} + \frac{\partial N_{xy}}{\partial x}\frac{\partial w_0}{\partial y} + \frac{\partial N_{xy}}{\partial y}\frac{\partial w_0}{\partial x} + \frac{\partial N_{yy}}{\partial y}\frac{\partial w_0}{\partial y} + \\ &F\cos(\Omega_1 t) + V\cos(\Omega_2 t) - c_3\dot{w}_0 \\ &= I_0\ddot{w}_0 + I_1\left(\frac{\partial \ddot{u}_0}{\partial x} + \frac{\partial \ddot{v}_0}{\partial y}\right) - I_2\left(\frac{\partial^2 \ddot{w}_0}{\partial x^2} + \frac{\partial^2 \ddot{w}_0}{\partial y^2}\right) \end{aligned} \tag{7}$$

式中:

$$\begin{Bmatrix} N_{\alpha\beta} \\ M_{\alpha\beta} \end{Bmatrix} = \int_{-h/2}^{h/2}\sigma_{\alpha\beta}\begin{Bmatrix} 1 \\ z \end{Bmatrix}\mathrm{d}z, (\alpha,\beta \text{ 分别代表 } x,y)$$

$$I_i = \sum_{k=1}^{N}\int_{z_k}^{z_{k+1}}\rho_k(z)^i\mathrm{d}z, \ (i=0,1,2) \tag{8}$$

将内力与应变关系带入到式(8)中,得到广义位移表示的复合材料层合悬臂板的控制方程如下:

$$\begin{aligned} &A_{11}\frac{\partial^2 u_0}{\partial x^2} + A_{66}\frac{\partial^2 u_0}{\partial y^2} + (A_{12}+A_{66})\frac{\partial^2 v_0}{\partial x\partial y} + A_{11}\frac{\partial w_0}{\partial x}\frac{\partial^2 w_0}{\partial x^2} + \\ &A_{66}\frac{\partial w_0}{\partial x}\frac{\partial^2 w_0}{\partial y^2} + (A_{12}+A_{66})\frac{\partial w_0}{\partial y}\frac{\partial^2 w_0}{\partial x\partial y} = I_0\frac{\partial^2 u_0}{\partial t^2} - I_1\frac{\partial^3 w_0}{\partial x\partial t^2} \end{aligned} \tag{9a}$$

$$\begin{aligned} &A_{22}\frac{\partial^2 v_0}{\partial y^2} + A_{66}\frac{\partial^2 v_0}{\partial x^2} + (A_{21}+A_{66})\frac{\partial^2 u_0}{\partial x\partial y} + A_{22}\frac{\partial w_0}{\partial y}\frac{\partial^2 w_0}{\partial y^2} + \\ &A_{66}\frac{\partial w_0}{\partial y}\frac{\partial^2 w_0}{\partial x^2} + (A_{21}+A_{66})\frac{\partial w_0}{\partial x}\frac{\partial^2 w_0}{\partial x\partial y} = I_0\frac{\partial^2 v_0}{\partial t^2} - I_1\frac{\partial^3 w_0}{\partial y\partial t^2} \end{aligned} \tag{9b}$$

$$\begin{aligned} &-D_{11}\frac{\partial^4 w_0}{\partial x^4} + (-D_{21}-4D_{66}-D_{12})\frac{\partial^4 w_0}{\partial x^2\partial y^2} - D_{22}\frac{\partial^4 w_0}{\partial y^4} + \frac{3A_{11}}{2}\cdot \\ &\left(\frac{\partial w_0}{\partial x}\right)^2\frac{\partial^2 w_0}{\partial x^2} + \frac{3}{2}A_{22}\left(\frac{\partial w_0}{\partial y}\right)^2\frac{\partial^2 w_0}{\partial y^2} + \left(\frac{1}{2}A_{21}+A_{66}\right)\cdot \end{aligned}$$

$$\left(\frac{\partial w_0}{\partial x}\right)^2\frac{\partial^2 w_0}{\partial y^2}+A_{11}\frac{\partial u_0}{\partial x}\frac{\partial^2 w_0}{\partial x^2}+\left(\frac{1}{2}A_{12}+A_{66}\right)\left(\frac{\partial w_0}{\partial y}\right)^2\frac{\partial^2 w_0}{\partial x^2}+$$

$$2\left(\frac{1}{2}A_{21}+2A_{66}+\frac{1}{2}A_{12}\right)\frac{\partial w_0}{\partial x}\frac{\partial w_0}{\partial y}\frac{\partial^2 w_0}{\partial x\partial y}+A_{22}\frac{\partial v_0}{\partial y}\frac{\partial^2 w_0}{\partial y^2}+$$

$$A_{21}\frac{\partial u_0}{\partial x}\frac{\partial^2 w_0}{\partial y^2}+A_{12}\frac{\partial v_0}{\partial y}\frac{\partial^2 w_0}{\partial x^2}+2A_{66}\frac{\partial u_0}{\partial y}\frac{\partial^2 w_0}{\partial x\partial y}+2A_{66}\frac{\partial v_0}{\partial x}\frac{\partial^2 w_0}{\partial x\partial y}+$$

$$\left(A_{21}+A_{66}\right)\frac{\partial w_0}{\partial y}\frac{\partial^2 u_0}{\partial y\partial x}+A_{11}\frac{\partial w_0}{\partial x}\frac{\partial^2 u_0}{\partial x^2}+\left(A_{12}+A_{66}\right)\frac{\partial w_0}{\partial x}\frac{\partial^2 v_0}{\partial y\partial x}+$$

$$A_{66}\frac{\partial w_0}{\partial x}\frac{\partial^2 u_0}{\partial y^2}+A_{66}\frac{\partial w_0}{\partial y}\frac{\partial^2 v_0}{\partial x^2}+A_{22}\frac{\partial w_0}{\partial y}\frac{\partial^2 v_0}{\partial y^2}-$$

$$N_{xx}{}^{p}\cos(\Omega_p t)\frac{\partial^2 w_0}{\partial x^2}-\left[p_0+p_1\cos(\Omega_3 t)\right]\frac{\partial^2 w}{\partial y^2}+$$

$$N_{yy}{}^{p}\cos(\Omega_p t)\frac{\partial^2 w_0}{\partial y^2}\left(\frac{\partial N_{xx}{}^{p}}{\partial x}\frac{\partial w_0}{\partial x}+\frac{\partial N_{yy}{}^{p}}{\partial y}\frac{\partial w_0}{\partial y}\right)+$$

$$F\cos(\Omega_1 t)+V\cos(\Omega_2 t)=c_3\dot{w}_0+I_0\ddot{w}_0-I_2\frac{\partial^2\ddot{w}_0}{\partial x^2}-$$

$$I_2\frac{\partial^2\ddot{w}_0}{\partial y^2}+\left(I_1\frac{\partial\ddot{u}_0}{\partial x}+I_1\frac{\partial\ddot{v}_0}{\partial y}\right) \tag{9c}$$

其中 $(A_{ij},B_{ij},D_{ij})=\sum_{k=1}^{N}\int_{z_k}^{z_{k+1}}(Q_{ij})_k(1,z,z^2)\,\mathrm{d}z$,$(i,j=1,2,6)$

2　Galerkin 离散

将悬臂板的模态函数写成悬臂梁与自由梁模态函数的组合[10],采用 Galerkin 方法,取 z 方向前四阶振型进行离散,选取模态函数如下:

$$u_0(x,y,t)=u_1(t)\sin\left(\frac{\pi x}{2a}\right)\cos\left(\frac{\pi y}{b}\right)$$

$$v_0(x,y,t)=v_1(t)\sin\left(\frac{\pi x}{2a}\right)\cos\left(\frac{\pi y}{b}\right)$$

$$w_0(x,y,t)=w_1(t)\alpha_1\beta_1+w_2(t)\alpha_1\beta_2+w_3(t)\alpha_2\beta_1+w_4(t)\alpha_2\beta_2$$

$$\alpha_1=\cosh\frac{k_1x}{a}-\cos\frac{k_1x}{a}-\varphi_1\left(\sinh\frac{k_1x}{a}-\sin\frac{k_1x}{a}\right)$$

$$\alpha_2=\cosh\frac{k_2x}{a}-\cos\frac{k_2x}{a}-\varphi_2\left(\sinh\frac{k_2x}{a}-\sin\frac{k_2x}{a}\right)$$

$$\cos k_i\cosh k_i+1=0,\ k_i{}^4=\omega^2\frac{\rho A}{EJ}\ (i=1,2)$$

$$\varphi_i=\frac{\sinh k_i-\sin k_i}{\cosh k_i+\cos k_i}\ (i=1,2)$$

$$\beta_1=1,\ \beta_2=\sqrt{3}\left(1-\frac{2y}{b}\right) \tag{10}$$

对于悬臂薄板,横向位移比其它方向的位移更加明显,因此忽略(9a)(9b)方程的所有惯性项和(9c)关于 u_0,v_0 的惯性项,利用 Galerkin 方法,将(10)带入到(9),得到 w_1,w_2,w_3,w_4 的表达式如下:

$$\ddot{w}_1+\mu_1\dot{w}_1+\omega_1^2w_1+a_1w_1{}^3+a_2w_2{}^3+a_3w_3{}^3+a_4w_4{}^3+a_5w_1w_2^2+a_6w_2w_1^2+a_7w_3w_2^2+a_8w_3w_1^2+a_9w_1w_3^2+a_{10}w_1w_4^2+a_{11}w_2w_3^2+a_{12}w_2w_4^2+a_{13}w_4w_2^2+a_{14}w_3w_4^2+a_{15}w_4w_1^2+a_{16}w_4w_3^2+a_{17}w_1w_2w_3+a_{18}w_1w_2w_4+a_{19}w_1w_3w_4+a_{20}w_2w_3w_4=a_{21}F\cos\Omega_1t+a_{22}V\cos(\Omega_2t)$$

$$\ddot{w}_2+\mu_1\dot{w}_2+\omega_2^2w_2+b_1w_1{}^3+b_2w_2{}^3+b_3w_3{}^3+b_4w_4{}^3+b_5w_1w_2^2+b_6w_2w_1^2+b_7w_3w_2^2+b_8w_3w_1^2+b_9w_1w_3^2+b_{10}w_1w_4^2+b_{11}w_2w_3^2+b_{12}w_2w_4^2+b_{13}w_4w_2^2+b_{14}w_3w_4^2+b_{15}w_4w_1^2+b_{16}w_4w_3^2+b_{17}w_1w_2w_3+b_{18}w_1w_2w_4+b_{19}w_1w_3w_4+b_{20}w_2w_3w_4=b_{21}F\cos\Omega_1t+b_{22}V\cos(\Omega_2t)$$

$$\ddot{w}_3+\mu_1\dot{w}_3+\omega_3^2w_3+c_1w_1{}^3+c_2w_2{}^3+c_3w_3{}^3+c_4w_4{}^3+c_5w_1w_2^2+c_6w_2w_1^2+c_7w_3w_2^2+c_8w_3w_1^2+c_9w_1w_3^2+c_{10}w_1w_4^2+c_{11}w_2w_3^2+c_{12}w_2w_4^2+c_{13}w_4w_2^2+c_{14}w_3w_4^2+c_{15}w_4w_1^2+c_{16}w_4w_3^2+c_{17}w_1w_2w_3+c_{18}w_1w_2w_4+c_{19}w_1w_3w_4+c_{20}w_2w_3w_4=c_{21}F\cos\Omega_1t+c_{22}V\cos(\Omega_2t)$$

$$\ddot{w}_4+\mu_1\dot{w}_4+\omega_4^2w_4+d_1w_1{}^3+d_2w_2{}^3+d_3w_3{}^3+d_4w_4{}^3+d_5w_1w_2^2+d_6w_2w_1^2+d_7w_3w_2^2+d_8w_3w_1^2+d_9w_1w_3^2+d_{10}w_1w_4^2+d_{11}w_2w_3^2+d_{12}w_2w_4^2+d_{13}w_4w_2^2+d_{14}w_3w_4^2+d_{15}w_4w_1^2+d_{16}w_4w_3^2+d_{17}w_1w_2w_3+d_{18}w_1w_2w_4+d_{19}w_1w_3w_4+d_{20}w_2w_3w_4=d_{21}F\cos\Omega_1t+d_{22}V\cos(\Omega_2t) \tag{11}$$

3　数值模拟

利用 Runge-Kutta 法,数值模拟电压激励对于系统非线性动力学响应的影响.选择压电层合悬臂板的实际物理参数如表 1,其中下脚标 s 代表基底层的相关参数,下脚标 p 代表压电层的相关参数,其它参数的代表意义与前述相同.

表 1　压电悬臂板的物理参数

Table 1　Physical parameters of the cantilevered plate

physical quantity	value	physical quantity	value
a	1.5m	E1p	2.5GPa
b	0.8m	E2p	2.5GPa
hs	0.005m	G12p	1.0GPa
hp	0.001m	ν_{12p}	0.35
E1s	125Gpa	ρ_p	2500 kg/m^3
E2s	7.2Gpa	e31	17co/m^2
G12s	4.0GPa	e32	6co/m^2
ν_{12s}	0.33	c_3	2.83×10^{-5}
ρ_s	1570kg/m^3		

代入表 1 的物理参数到方程(11),并选取基础激励的幅值 $F=200$N,根据之前所做分析,当基础激励幅值 $F=200$N 时,系统响应为混沌,选择电压激励的幅值从 150V 变化到 10V 时,观察系统前二阶非线性动力学响应的变化如分叉图 2 所示.图中 w_1、w_2 分别代表前二阶响应的幅值.由图可知,当电压达到 90V 时,系统响应由混沌运动变为周期运动,降低了振幅,达到了抑制振动的效果.

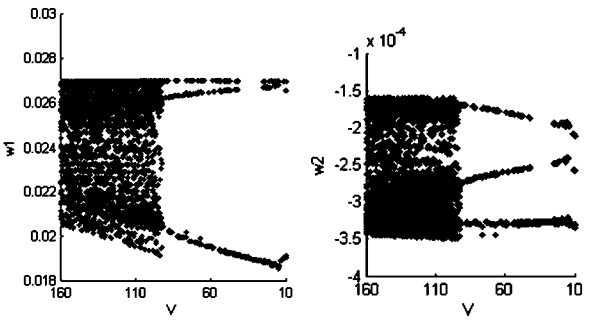

图 2 系统前二阶模态随电压幅值变化的分叉图

Fig.2 Bifurcation diagram of the first four modes for w_0 under the voltage excitation V

选取电压激励的幅值 120V 时,得到系统的波形图(a),二维相图(b),庞加莱截面(c)和三维相图(d),如图 3 所示.图中 x_1 代表第一阶的振幅,x_2 代表第一阶的速度.从图 3 可以看出,系统运动为混沌.

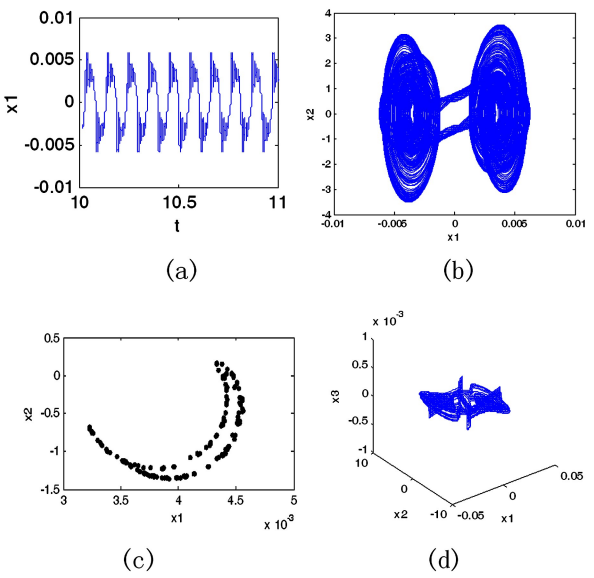

图 3 当 $V=120$V 系统的混沌运动

Fig.3 Chaotic motion of the system when $V=120$V

选取电压激励的幅值为 50V 时,得到系统的波形图(a),二维相图(b),庞加莱截面(c)和三维相图(d),如图 4 所示.从这些图可以看出,系统运动为倍周期.

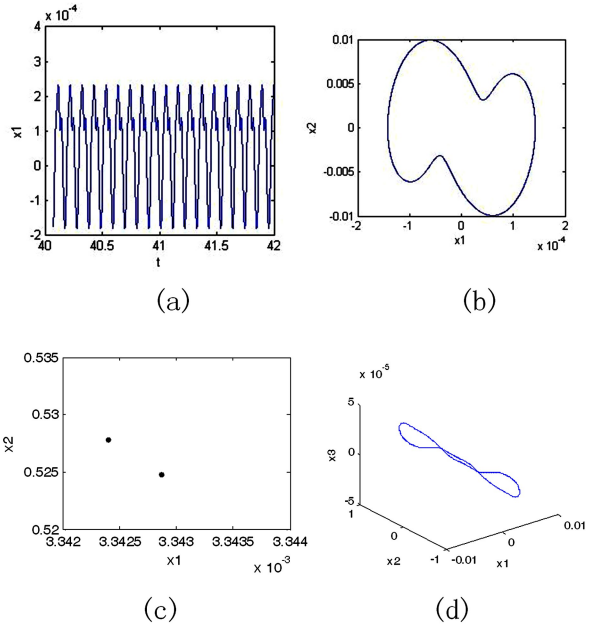

图 4 当 $V=50$V 系统的倍周期运动

Fig.4 Periodic motion of the system when $V=50$V

4 结论

本文研究了在基础激励、电压激励和面内激励联合作用下,复合材料层合压电悬臂板的非线性动力学响应.应用经典板理论和 Hamilton 原理建立系统动力学方程,采用 Galerkin 方法对系统进行四阶离散,代入实际物理参数,数值模拟得到振动幅值随电压激励变化的分叉图,由图可知,通过给系统施加电压激励,产生逆压电效应,系统响应由大幅值的混沌运动变为幅值较小的倍周期运动,抑制了系统的振动.实际工程中,飞行器在高速飞行时,其机翼由于振动会产生疲劳甚至破坏,而利用压电材料的逆压电效应,通过选择合适的电压激励的幅值,能够抑制机翼的振动,保持系统的稳定.

参 考 文 献

1 栾桂冬,张金铎,王仁乾.压电换能器和换能器阵. 北京:北京大学出版社, 2005 (Luan G D, Zhang J D, Wang R Q. Piezoelectric transducer and transducer array. Beijing: Peking University Press, 2005 (in Chinese))

2 Zhang W. Global and chaotic dynamics for a parametrically excited thin plate. *Journal of Sound and Vibration*,

2001,239(5):1013~1036

3 Yu P, Zhang W, Bi Q S. Vibration analysis on a thin plate with the aid of computation of normal forms. *International Journal of Non-linear Mechanics*, 2001,36:597~627

4 Hao Y X, Chen L H, Zhang W, et al. Nonlinear oscillations bifurcations and chaos of functionally graded materials plate. *Journal of Sound and Vibration*, 2008,312:862~892

5 姚志刚,张伟,陈丽华. 压电复合材料层合梁的分叉、混沌动力学与控制研究. 力学学报, 2009,41:129~140 (Yao Z G, Zhang W, Chen L H. The nonlinear oscillation, bifurcation and chaotic dynamics of a simply supported laminated composite piezoelectric beam. *Chinese Journal of Theoretical and Applied Mechanics*, 2009, 41:129~140 (in Chinese))

6 Arrieta A F, Hagedorn P, Erturk A, et al. A piezoelectric bistable plate for nonlinear broadband energy harvesting. *Applied Physics Letters*, 201097:102~104

7 Betts D N, Bowen C R, Kim H A, et al. Nonlinear static response of piezoelectric plates considering electro-mechanical coupling. *The European Physical Journal Special Topics*, 2013,222:1553~1562

8 李蒙. 复合材料点阵夹芯板壳振动主动控制研究[硕士学位论文]. 北京: 北京工业大学, 2016 (Li M. Active vibration control of composite lattice sandwich plates and shells[Master Thesis]. Beijing: Beijing University of Technology, 2016(in Chinese))

9 Reddy J N. Mechanics of laminated composite plates and shells: Theory and Analysis. Boca Raton: CRC Press LLC,2004

10 Zhang W, Zhao M H. Nonlinear vibrations of a composite laminated cantilever rectangular plate with one-to-one internal resonance. *Nonlinear Dynamics*, 2012,70:295~313

BIFURCATIONS OF A COMPOSITE LAMINATED CANTILEVERED PLATE UNDER VOLTAGE EXCITATION*

Yang Jiahui[1,2]　Zhang Wei[1†]　Yao Minghui[1]　Yu Tianjun[1]

(1. *College of Mechanical Engineering*, *Beijing University of Technology*, *Beijing* 100124, *China*)

(2. *Beijing Vocational College of Agriculture*, *Beijing* 102208, *China*)

Abstract The bifurcations of a composite laminated cantilevered plate are studied, which is simultaneously forced by the voltage, base and in-plane excitations. The nonlinear partial differential governing equations of the system motion are established by using the Hamilton's principle. The Galerkin approach is used to discretize the partial differential equations to the ordinary differential equations with four degree of freedom. Numerical simulations are also carried out to investigate the effects of the voltage excitation on the steady-state responses of the cantilevered piezoelectric plate. The bifurcation diagram of the system is then obtained. The system motions can be shown as follows: the chaotic motion to the multiple periodic motion. The results show that the amplitude of the system can reduce effectively and keep the stability by adjusting the voltage excitation.

Key words cantilever plate, Hamilton's principle, bifurcation, nonlinear dynamics, chaos

Received 29 December 2016, revised 24 January 2017.

* The project supported by the National Natural Science Foundation of China(11290152,11322214).

† Corresponding author E-mail: sandyzhang0@yahoo.com